Journal of Pharmaceutical and Biomedical Analysis 55 (2011) 114–124

Contents lists available at ScienceDirect

Journal of Pharmaceutical and Biomedical Analysis

journal homepage: www.elsevier.com/locate/jpba

# Lomefloxacin promotes the interaction between human serum albumin and transferrin: A mechanistic insight into the emergence of antibiotic's side effects

JamshidKhan Chamani[a,*], Hanif Vahedian-Movahed[a,b], Mohammad Reza Saberi[c]

[a] Department of Biology, Faculty of Sciences, Islamic Azad University-Mashhad Branch, Mashhad, Iran
[b] Islamic Azad University-Mashhad Branch, Young Researcher Club, Mashhad, Iran
[c] Department of Medical Chemistry, School of Pharmacy, Mashhad University of Medical Sciences, Mashhad, Iran

ARTICLE INFO

*Article history:*
Received 4 September 2010
Received in revised form
15 December 2010
Accepted 18 December 2010
Available online 31 December 2010

*Keywords:*
Protein–protein interaction
Albumin
Transferrin
Lomefloxacin

ABSTRACT

Human serum albumin (HSA) and serum transferrin (TF) are two drug carrier proteins *in vivo*. In this study it was investigated how lomefloxacin (LMF) binding affected the HSA–TF interaction using different spectroscopic, calorimetric and molecular modeling techniques. Fluorescence, circular dichroism and synchronous fluorescence revealed that LMF could bind to both proteins, resulting in protein conformational changes. Moreover, HSA and TF could interact so that some fluorescence residues were positioned at the interface and were shielded from quenching by LMF. The interaction between HSA and TF was further confirmed by fluorescence resonance energy transfer. Quantitative analyses of the far-UV CD spectra of the HSA–TF interaction in the presence and absence of LMF revealed secondary structural changes in detail. Resonance light-scattering studies demonstrated that the HSA–TF interaction resulted in a new species with a larger size, and that the presence of LMF could further favor this reaction. Isothermal titration calorimetry revealed that electrostatic interaction was dominant in the absence of LMF, whereas van der Waals forces and hydrogen bonding become significant in its presence. On the other hand, it was found that the binding constant of TF bound to HSA was stronger in the presence of LMF. ANS fluorescence further indicated that hydrophobic interactions play a minor part in the HSA–TF system. Molecular modeling studies confirmed the presence of fluorophore residues, hydrogen bonding and electrostatic interactions at the interface of the HSA–TF complex. It also suggested that the binding sites of LMF were not located there. These data indicate that LMF can modify the interaction between HSA and TF as two model proteins present in serum. The relevance to drugs' side effects, pharmacokinetic of drugs and selection of diagnostic biomarker is discussed.



## 1. Introduction

Protein–protein interaction (PPI) has an essential role in sustaining many biological processes such as signal transduction, regulation of enzymatic activities, immune response, and assembly of cellular components [1]. PPI is therefore considered to be a potential drug target [2]. Loss or gain of PPI is considered to be associated with several human diseases, including bare lymphocyte syndrome, which is related to loss of PPI, and Wermer's syndrome, which is related to the gain of PPI. PPI could be the first step in protein aggregation. Aggregate formation is often triggered by minor induced-conformational changes and is correlated to the development of neurodegenerative diseases [3]. Some investigations demonstrated that non-disease-related proteins can also be induced to form amyloid fibrils and can be cytotoxic to non-neuronal cells [4]. They can also induce immunogenic responses [5]. Moreover, aggregation is a problem in over expression of recombinant proteins in biotechnology, and can potentially limit the half-life of the final product in the pharmaceutical industry [6]. A better understanding of PPI can also be useful in estimation of salt-induced protein precipitation, and in the crystallography of proteins [7]. Apart from these relationships to disease and industrial applications, PPI is also of importance in the self-assembly of proteins into supra-molecular structures for the development of tools in the nm–μm scale [8].

Understanding the various molecular factors and principles governing PPI could therefore be of great importance in biotechnological, pharmaceutical, industrial, cellular and medical researches. The effect of co-solvent, mutation, temperature, pH, ionic strength and ligands on PPI has been studied [1,9]. In the case of ligands, it is known that the protein–protein association constant can be coupled to the ligand–protein association constant as evidence for dimer–tetramer equilibrium of fully bound and ligand-free hemoglobin [10].

* Corresponding author. Tel.: +98 511 8437107; fax: +98 511 8424020.
*E-mail addresses:* Chamani@ibb.ut.ac.ir, Chamani.j@yahoo.com (J. Chamani).

0731-7085/$ – see front matter © 2010 Elsevier B.V. All rights reserved.
doi:10.1016/j.jpba.2010.12.029

Serum constitutes a network of PPI in which the most abundant proteins such as human serum albumin (HSA) and serum transferrin (TF) may act as "molecular sponges" which bind and transport hormones, lipoproteins and other proteins [9], as well as other extrinsic or intrinsic ligands such as bilirubin, drugs and minerals. Characterization of the interaction of drug molecules with such proteins therefore constitutes a key step in drug development [11]. However, most studies have focused on proteins separated from their partners and have overlooked the presence of other proteins. Studies attempting to elucidate if a drug molecule can change serum PPI are lacking.

In the present study, the focus was on the effect of lomefloxacin (LMF) on the interaction between two drug carrier proteins: HSA and TF. LMF is a third-generation fluoroquinolone antibiotic that exhibits striking potency against a broad spectrum of Gram-negative and Gram-positive bacteria through inhibition of DNA gyrase [12]. This antibiotic is efficacious in the treatment of bronchitis and infections of the urinary tract. However, it has side effects: central nervous system (CNS) affects, peripheral edema, phototoxicity and, rarely, discoloration of skin, yellow eyes or skin, and it has increased the incidence of fetal loss in monkeys [12]. There have been numerous reports on the interaction of LMF with serum proteins such as HSA and TF [13]. However its effect on PPI has not been reported.

HSA is a single-chain, largely α-helical protein composed of 585 amino-acid residues which constitute ~60% of total plasma protein ($\leq$40 mg mL$^{-1}$). It is composed of three structurally homologous domains (I–III) which are further divided into two sub-domains (A and B) that are arranged in a heart-shaped structure. In addition to functioning as a carrier, this protein is also responsible for the regulation of colloidal osmotic pressure, maintenance of blood pH, and is a possible source of amino acids for different tissues [14].

TF is a single-chain protein containing 679 amino acid residues with a serum concentration of 2.5 mg mL$^{-1}$. This protein is divided into two lobes (N and C), each of which contains two domains comprising a series of α-helices and β-sheets. This "multi-task protein" is also involved in growth, differentiation, cytoprotection, and antimicrobial activities apart from its tasks of metal binding and transportation [15]. Several reports on the interaction of TF with different drugs have also been published [13].

The present study was aimed at elucidating, if a drug molecule can change the PPI between two serum carrier proteins. This phenomenon could have important consequences. First, it can affect the natural function of both proteins. For example, it can reduce the bilirubin binding to HSA and cause hyperbilirubinemia [16] or, provided PPI proceeds by aggregation, it can reduce the concentration of HSA and may cause edema through reducing the colloidal osmotic pressure [17] (similar to some of the observed side effects for LMF) and may also induce the immune response. Therefore, it may provide new insights into the observed side effects of the drug. Second, the binding parameters of drugs to carrier proteins can be influenced. These parameters are usually determined on a protein separated from its partner, and the effect of other protein interactions is often ignored. Third, protein interaction with other proteins or ligands which are used as biomarkers can be altered [9] for clinical application. This may lead to false-negative or false-positive results which could be important for future diagnostic tests. In general, the present study could strengthen our understanding of the effect of drugs on PPI and its consequences.

The effect of LMF on the interaction between HSA and TF was investigated using intrinsic tryptophan (Trp), extrinsic 1-anilinonaphthalene-8-sulphonate (ANS), second-derivative and synchronous fluorescence, resonance light scattering (RLS), fluorescence resonance energy transfer (FRET), isothermal titration calorimetry (ITC), circular dichroism (CD) and molecular modeling. The results indicated that HSA and TF have interactions, and that LMF can strengthen this interaction.

## 2. Materials and methods

### 2.1. Materials

LMF, HSA, TF, ANS, potassium phosphate buffer and protoporphyrin IX (PPIX) were purchased from Sigma–Aldrich (St. Louis, MO, USA). Dimethyl formamide (DMF), sodium carbonate, ethylenediamine tetra-acetic acid (EDTA), ethanol and sodium hydroxide were obtained from Merck chemical Co. (Germany). Visking® dialysis tubing was procured from Scientific Instrument Center Limited (SIC, Eastleigh, UK). All materials were used without further purification. Double-distilled water was used throughout the experiments.

### 2.2. Sample preparation

All protein solutions were freshly prepared in potassium phosphate buffer (50 mM, pH 7.4). LMF (0.025 mM) stock solution was prepared by dissolving in the same buffer and storing in a refrigerator at 4 °C in the dark. A digital pH-meter (Metrom, Berlin, Germany) was used for pH adjustment.

### 2.3. Methods

#### 2.3.1. Intrinsic, extrinsic and second-derivative fluorescence spectroscopy

Fluorescence spectra were recorded on a F-2500 spectrofluorometer (Hitachi, Tokyo, Japan) linked to a personal computer and equipped with a 150-W xenon arc lamp, gating excitation and emission monochromators, and a Hitachi recorder. Slit widths for both monochromators were set at 10 nm. A 3-cm quartz cell was used. A 2.0-mL solution containing an appropriate concentration of plasma proteins (separately or mixed) was titrated manually by successive addition of a 0.025-mM stock solution of LMF (final concentration, $6.23 \times 10^{-5}$–0.002 mM) with trace syringes. Intensity was recorded for Trp and ANS fluorescence. The excitation wavelength for Trp was 280 nm and the emission wavelength was 300–600 nm. To decrease the inner filter effect, the fluorescence intensities used in the present study were corrected for absorption of the excitation light and re-absorption of emitted light using the formula:

$$F_{cor} = F_{obs}\, e^{(A_{ex}+A_{em})/2}$$

where $F_{cor}$ and $F_{obs}$ are the corrected fluorescence intensity and observed fluorescence intensity, respectively, and $A_{ex}$ and $A_{em}$ are the absorption of the system at the excitation wavelength and at the emission wavelength, respectively [18]. ANS fluorescence was measured at 370–700 nm using an excitation wavelength of 350 nm with the final concentration of the dye of $5 \times 10^{-3}$ mM. Second-derivative spectra were also obtained from the original peaks of Trp fluorescence. In all titration experiments, the dilution factor of ligand titration was corrected.

#### 2.3.2. RLS and synchronous fluorescence

For RLS measurement, the excitation and emission monochromators were scanned simultaneously with $\Delta\lambda = 0$ nm from 220 nm to 800 nm with the same instrument used for fluorescence measurements. A 2-mL solution containing $4 \times 10^{-3}$ mM HSA was injected successively by 40 aliquots of 5 μL of 0.1 mM TF solution to obtain a final concentration of TF ranging from $2.5 \times 10^{-2}$ to $9.1 \times 10^{-3}$ mM (TF/HSA molar ratio of 0.06–2.28). An identical procedure was carried out in concentrations of 0.001, 0.002 and 0.003 mM of LMF. Synchronous fluorescence spectra were

obtained by simultaneously scanning the excitation and emission monochromators. Synchronous fluorescence spectra are characteristics of the tyrosine and tryptophan residues of HSA and TF when the wavelength interval ($\Delta\lambda$) is 15 nm and 60 nm, respectively. In all titration experiments, the dilution factor of the ligand titration was corrected.

*2.3.3. FRET*

HSA was labeled by PPIX as the acceptor probe according to a previously described method [19]. A 2-mL solution containing 4 μM HSA–PPIX was titrated successively by 20 aliquots of 10 μL of 0.1 mM TF solution to obtain a final concentration of TF ranging from $5 \times 10^{-4}$ to $9.10 \times 10^{-3}$ mM (TF/HSA molar ratio of 0.12–2.28). The excitation wavelength was set at 297 nm and the emission wavelength was 300–800 nm using the same instrument employed for fluorescence measurements. The same procedure was carried out for 0.001, 0.002 and 0.003 mM of LMF. The dilution factor of the ligand titration was also corrected.

*2.3.4. ITC*

Calorimetric measurements were carried out using a Nano-ITC machine (TA Instruments Limited, New Castle, DE, USA). The sample cell was loaded with 1 mL of HSA ($4 \times 10^{-3}$ mM) and the reference cell contained double-distilled water. To examine the effect of LMF, it was added to the sample cell containing HSA and also to the reference cell. Titration was carried out using a 250-μL syringe filled with TF solution at 298 K, while the contents of the cell were stirred at 400 rpm.

Generated heats of binding were measured over 25 successive injections (injection volume, 5 μL) of 12-s duration each with an interval of 300 s between each injection. The integrated heat of injection was corrected by subtraction of the heat of dilution obtained by titration of TF into the buffer alone and buffer + LMF. The heat evolved per mole of TF injection was plotted against the molar ratio of TF to HSA. Data were fitted to a single set of identical site model using ITC Run software supplied with the instrument. Accordingly, the molar enthalpy change for the binding ($\Delta H^0$), the binding stoichiometry ($n$), and binding constant ($K_b$) were obtained. The molar free energy change ($\Delta G^0$) and the molar entropy change ($\Delta S^0$) for the binding were obtained using the fundamental thermodynamic equations [20,30]:

$$\Delta G^0 = -RT \ln K_b$$

$$\Delta S^0 = \frac{\Delta H^0 - \Delta G^0}{T}$$

*2.3.5. CD*

Far-ultraviolet (UV) CD experiments were carried out on a Jasco-815 spectropolarimeter (Jasco, Tokyo, Japan) equipped with a Jasco 2-syringe titrator under constant nitrogen flush at room temperature. The instrument was controlled by Jasco Spectra Manager™ software. The scanning rate, bandwidth, and response were set at 50 nm $min^{-1}$, 1 nm and 2 s, respectively. The instrument was calibrated using *d*-10-camphorsulphonic acid. A quartz cuvette with a path length of 1 mm was used. Each spectrum was the mean of five successive scans with a protein concentration constant of $1.33 \times 10^{-3}$ mM and $1.26 \times 10^{-3}$ mM for HSA and TF, respectively.

For exploring changes in secondary structure, far-UV CD spectra were obtained over a wavelength range of 190–240 nm in the absence and presence of different concentrations of LMF at the same conditions as described above for HSA and TF solutions, separately. In addition, a 2-mL solution containing HSA ($1.33 \times 10^{-3}$ mM) was injected successively by 10 aliquots of 20 μL of $33.5 \times 10^{-3}$ mM TF solution to obtain a final concentration of TF ranging from $0.33 \times 10^{-3}$ to $3.04 \times 10^{-3}$ mM (TF/HSA molar ratio of 0.25–2.28). The same procedure was repeated in the presence of 0.001, 0.002 and 0.003 mM of LMF. In all titration experiments, the dilution factor of the ligand titration was corrected.

*2.3.6. Homology modeling of holo-TF*

A homology-based model of human holo-TF was generated using the crystal structures of the N-lobe of human holo-TF (PDB code 1D3K) and rabbit holo-TF (PDB code 1JNF) as templates. These templates were identified according to PSI-BLAST homology searches against available pdb structures. Model building was undertaken in the program modeler 9v7® (http://salilab.org/modeler/) using a multiple model algorithm. The predicated models were analyzed by Swiss-pdb-Viewer4® (http://www.expasy.org/spdbv) and web Lab-ViewrLite® (http://sunfire.vbi.vt.edu/gcg/seqweb-guides/WebLab_Viewer.html). The overall qualities of the models were then accessed using the ERRAT, VERIFY3D and Ramachandran plot at the UCLA server (http://nihserver.mbi.ucla.edu/savs/). According to evaluation scores, the models were refined and energy-minimized (by HyperChem 7® (http://www.hyper.com)) until the best structure was achieved.

*2.3.7. Molecular modeling and docking*

The docking calculations for LMF association with HSA and TF were undertaken using the autodock4 program (http://www.scripps.edu/pub/olson-web/doc/autodock/). The crystal structure of HSA was retrieved from the RCSB Protein Data Bank (PDB entry: 1ao6). For differic TF, a homology-based model was generated using modeler 9v7 (http://salilab.org/modeler/). The protein–protein docking program HEX v.5.1® [21] was subsequently used to examine plausible modes of interaction between HSA and TF. Briefly, HEX carries out a global rotational and translational space scan using spherical polar Fourier correlations, which rank the candidate low-energy conformations according to surface complementarily and electrostatic characteristics. Moreover, to model the effect of LMF on the interaction mode between HSA and TF, the complexes of HSA–LMF and TF–LMF (obtained from the best docking results) were submitted to energy minimization with $MM^+$ force field (http://www.hyper.com). The same energy minimizations were carried out on HSA and TF for protein–protein docking in the absence of LMF. Finally, the best docking results were submitted to web Lab-ViewrLite® (http://sunfire.vbi.vt.edu/gcg/seqweb-guides/WebLab_Viewer.html). Molegro Molecular Viewer® (http://www.molegro.com/mmv-product.php) and Swiss-pdb-Viewer4® (http://www.expasy.org/spdbv) for further analyses.

## 3. Results and discussion

### 3.1. Fluorescence quenching

The balance between the intermolecular forces responsible for protein conformation can be modified upon drug binding, leading to structural changes within the protein [22]. Therefore, the first step to study the effect of LMF on PPI is to characterize its interaction toward each protein separately.

Fluorescence spectroscopy was used to measure the interaction between LMF and HSA; LMF and TF; and mixture of both proteins. In all cases, fluorescence intensity was quenched by the addition of LMF to the protein solution but to different degrees (Fig. 1a and b).

The percentage of quenching for each system is illustrated in Fig. 1b: the quenching for HSA is much stronger than that observed in TF. However, when proteins were mixed together, the observed quenching was weaker than what would be expected from their algebraic average. This difference suggests that the accessibility of drugs to its binding sites may be limited by the formation of

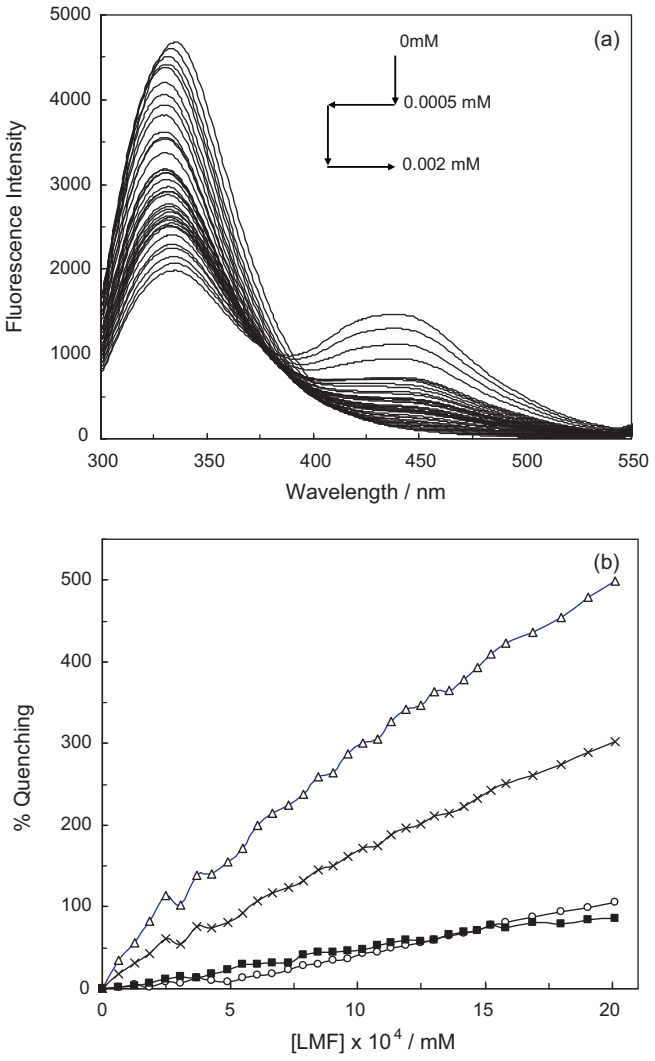


**Fig. 1.** Fluorescence emission spectra of the HSA–TF mixture in the presence of various concentrations of LMF (a). Percentage of quenching of HSA (△), TF (○), HSA–TF (□) and algebraic average of HSA–TF (×) in the presence of various concentrations of LMF (0–0.002 mM) (b). The concentrations of HSA, TF and HSA–TF were $4.5 \times 10^{-3}$ mM, $3.7 \times 10^{-3}$ mM and $4.5 \times 10^{-3}$ mM, respectively. $\lambda_{ex}$ = 280 nm; $T$ = 298 K; pH 7.4; phosphate buffer (50 mM).

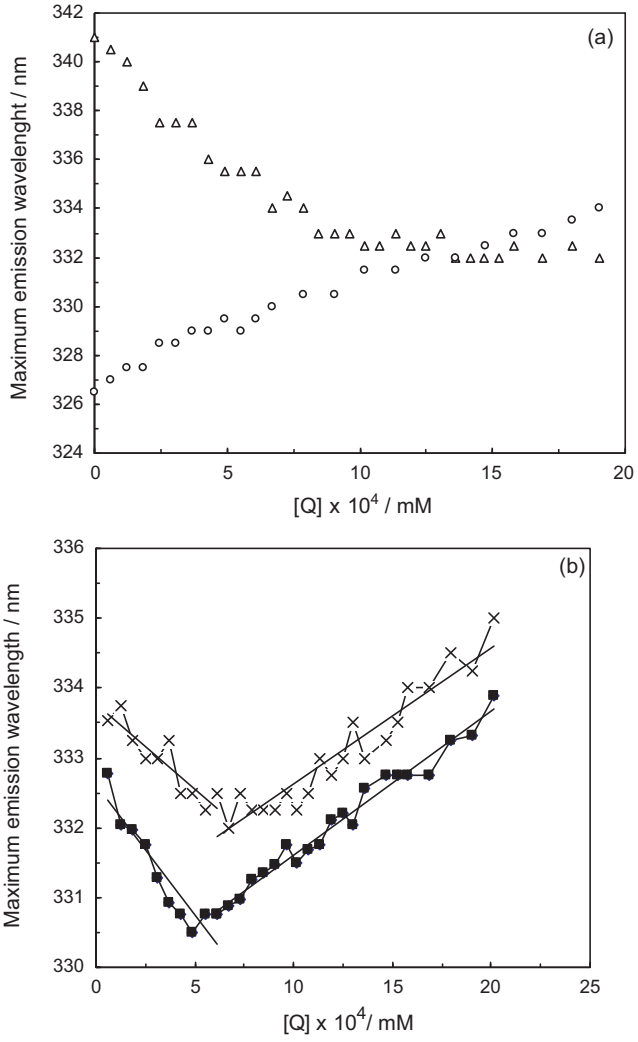


**Fig. 2.** Effect of LMF on the wavelength maxima of the intrinsic fluorescence emission spectra of proteins. (a) HSA (△) and TF (○). (b) HSA–TF (□) and algebraic average of HSA–TF (×).

a protein–protein complex. It is probable that a part of the binding site or some corridors which end at the binding site of drug are buried in the interface of the formed complex, or that structural changes in the protein have led to the destruction of binding sites. For the sake of illumination the number of binding sites ($n$) of LMF in each of the three systems and for the algebraic average of HSA–TF was obtained according to the Hill formula (Eq. (1)) [18]:

$$\log \frac{F_0 - F}{F} = \log K_a + n \log[L] \quad (1)$$

where $F$ and $F_0$ are the fluorescence intensities in the presence and absence of drug, respectively, $n$ is the number of binding sites, and $K_a$ is the binding constant. For HSA and TF, the $n$ value was found to be 0.77 and 1.02, respectively. However, for their mixture, it was 1.13, which is far smaller than the value expected from their algebraic average ($n$ = 1.81). This observation further confirms the conclusion stated above that a part of the binding site of the drug or some corridors which end at the binding sites are concealed upon protein–protein association or structural changes within the protein have led to destruction of the binding sites. The latter hypothesis has been confirmed by molecular modeling studies (see below). Therefore, the binding parameters of drugs to serum proteins can be affected by the presence of other function-related proteins present in serum.

Another finding that can be deciphered from the fluorescence spectra is the polarity of the local environment of Trp, which is reflected in the shifts of the maximum emission wavelength ($\lambda_{em,max}$), known as "Stoke's shifts" [18]. This is an elegant tool with which to study the formation of protein complexes. Fig. 2a shows that the interaction of LMF with HSA and TF led to a blue shift and a red shift in their $\lambda_{em,max}$, respectively. These observations indicate that the fluorescence residues of proteins are transferred to a more or less hydrophobic environment in case of HSA and TF, respectively, and that the conformation of the protein has been changed after interacting with LMF. Interestingly, a combination of blue shift and red shift in $\lambda_{em,max}$ was observed for a mixture of both proteins (Fig. 2a and b). This is unsurprising because the same trend was observed for their algebraic average. However, this was more "blue-shifted" for the mixture of HSA–TF compared with the computed average. This indicated that the PPI occurred and the fluorescence residues of proteins are located in the interface of the formed complex or transferred to a more hydrophobic environment within the protein.

One question remained to be answered: why did the blue shift precede the red shift in Fig. 1a. Comparing the quenching efficiency of each protein by LMF may help to answer this question.

The fluorescence dynamic quenching is usually analyzed by the Stern–Volmer equation (Eq. (2)) [18]:

$$\frac{F_0}{F} = 1 + K_{SV}[Q] = 1 + k_q\tau_0[Q] \quad (2)$$

where $F$ and $F_0$ are the fluorescence intensities in the presence and absence of drug, respectively; $K_{SV}$ is the Stern–Volmer quenching constant; [Q] is the concentration of the quencher; $k_q$ is the bimolecular quenching constant; and $\tau_0$ is the average lifetime of the biomolecule in the absence of the quencher ($\sim 10^{-8}$ for most biomolecules) [18]. The results show that the $K_{SV}$ value for HSA is about fourfold larger than of that for TF. Therefore, in the concentration range 0–$5 \times 10^{-4}$ mM, the quenching of HSA is dominant due to the stronger affinity of LMF for HSA. However, in the range $5 \times 10^{-4}$–$2 \times 10^{-3}$ mM, the quenching for TF is preferred until it becomes saturated. Also, the bimolecular quenching constant for HSA and TF is much greater than the maximum scatter collision constant of various types of quencher by biomolecules ($2 \times 10^{12}$ L mol$^{-1}$ s$^{-1}$) [18]. This suggests that quenching mainly resulted from static quenching (complex formation) rather than by dynamic (collision) quenching.

### 3.2. Second-derivative fluorescence spectroscopy

Second-derivative fluorescence spectra were obtained to monitor the micro-environmental transition of the fluorophores in the protein that takes place upon interaction with drugs and during PPI (Fig. 3). This technique enables characterization of even small changes in the local environment of the Trp and Tyr (when excited at 280 nm) of proteins which may not be obvious in conventional fluorescence spectra [22]. The spectra for HSA exhibited a single band in the range 320–350 nm which is due to the presence of only one Trp (Trp 214) in its structure. However, the spectra for TF (which is a multi-Trp protein) and mixture of HSA and TF exhibited double minima at the same wavelength region. This can be attributed to the presence of Trp in different microenvironments with different hydrophobicity [23]. Moreover, for TF, the percentage loss in intensity at those two bands did not follow the same trend, which indicates that the microenvironment of Trps is affected by different degrees (Fig. 3b). However, the percentage loss in intensity at these two bands for HSA–TF mixtures was much less than their algebraic average. Also, the trends in reduction for the two bands in HSA–TF mixtures were more dissimilar than that in their algebraic average. It is likely that protein–protein association weakened the effect of the drug on proteins, and the fluorescence residues were sequestered due to direct contact with the drug (Fig. 3b).

Moreover, the value of $H$ (which is indicative of the relative hydrophobicity of the Trp local environment) was calculated from second-derivative spectra according to the method of Mazo-Villarias [22]. Fig. 3c illustrates the obtained $H$ factor as a function of LMF concentration for HSA–TF mixtures and their algebraic average. From Fig. 3c it can be deduced that for HSA–TF mixture the fluorescence residues are lying in a more hydrophobic environment (possibly by PPI) and that the drug molecules could promote this by the order of 1.7 (calculated from the slope of the graph).

### 3.3. Synchronous fluorescence spectroscopy (SFS)

The observation that the HSA and TF conformations were affected by the addition of LMF was also illustrated by SFS. SFS was first introduced by Lloyd [24]. SFS provides information about the microenvironment in the vicinity of the chromophore species.

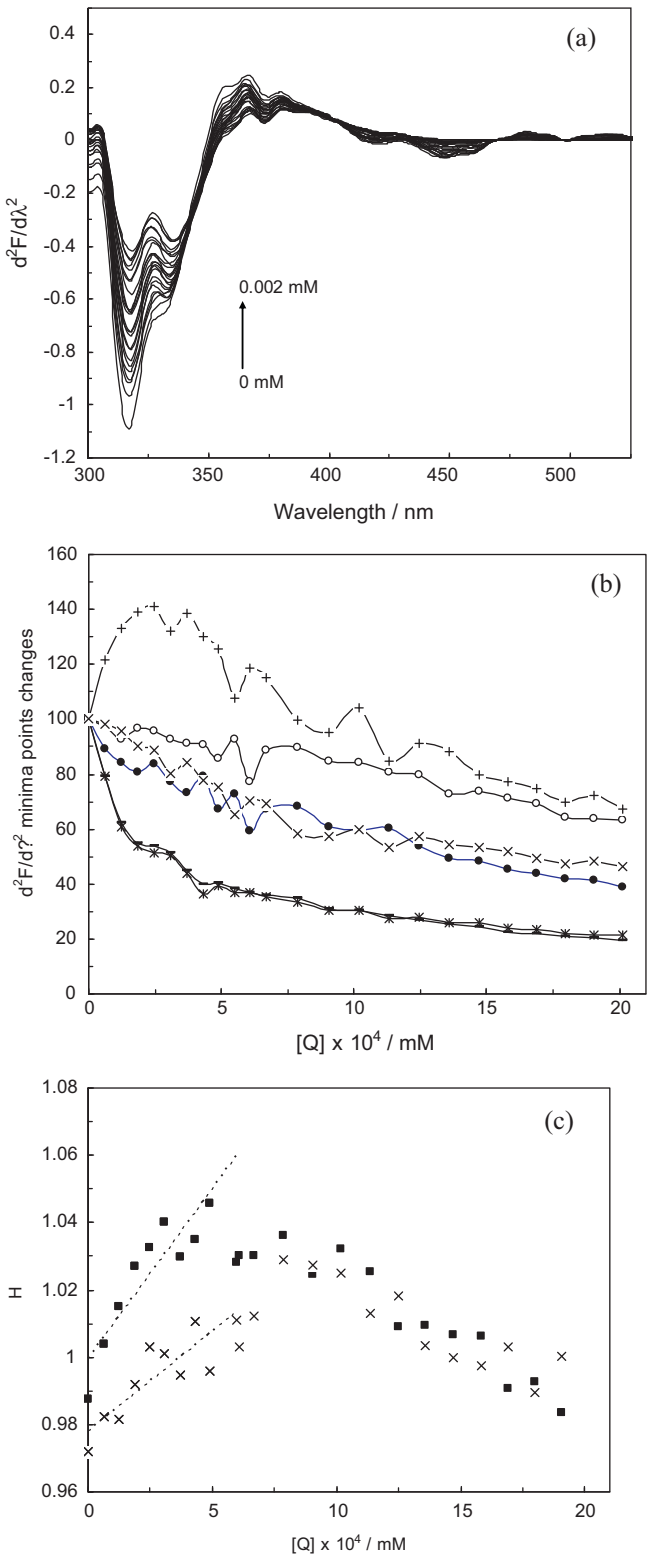


**Fig. 3.** (a) Fluorescence second-derivative spectra of HSA–TF treated by various concentrations of LMF at an excitation wavelength of 280 nm. (b) Effect of LMF on the percentage loss in intensity at first and second minima bands in the 315–340-nm region in fluorescence second-derivative spectra. TF (●, min 1; ○, min 2) HSA–TF (+, min 1; ×, min 2), algebraic average of HSA–TF (—-, min 1; *, min 2). (c) Effect of LMF on the relative hydrophobicity of the Trp local environment in HSA–TF (□) and algebraic average of HSA–TF (×).

In SFS, the sensitivity associated with fluorescence is maintained while providing other advantages such as spectral simplification, reduction in spectral bandwidth, and avoidance of various perturbing effects. If the interval between excitation and emission wavelengths ($\Delta\lambda$) is set at 15 nm and 60 nm, respectively, it provides characteristic information regarding Trp and Tyr residues, respectively [24]. It was evident that for HSA the $\lambda_{em,max}$ did a slight red shift and a blue shift when $\Delta\lambda$ was 15 nm and 60 nm, respectively. This indicates that the hydrophobicity around Trp decreased whereas for Tyr it increased. Also, for TF the $\lambda_{em,max}$ did a slight blue shift and red shift when $\Delta\lambda$ was 15 nm and 60 nm, respectively. This suggests that the hydrophobicity around Trp increased whereas for Tyr it decreased. These observations suggest that the conformations of both proteins changed upon interaction with LMF.

### 3.4. FRET

In the sections above, by measuring the changes in the polarity of the Trp microenvironment to some extent, it was demonstrated that HSA and TF could interact with each other. However, both proteins have the same excitation wavelength, so it was not possible to show this phenomenon by quenching experiments. In this section, to ensure that the conclusions detailed above are reliable, the interaction of HSA with TF through FRET was investigated. According to FRET theory [25], energy will be transferred from a donor to an acceptor provided that the following conditions are met: (a) the donor can produce fluorescent light; (b) the fluorescence spectrum of the donor overlaps the UV–vis absorption spectrum of the acceptor; (c) the distance between the donor and acceptor pair (TF and HSA, respectively, in the present study), is <7 nm. HSA was labeled by the extrinsic probe protoporphyrin IX (PPIX) to act as an acceptor. It is known that PPIX binds to the domain-IB of HSA [19] and that it can quench the fluorescence of Trp 214 through FRET because the emission spectrum of Trp overlaps with the absorption spectrum of PPIX and the spectral characteristics of PPIX appear at longer wavelengths. This has been studied by Kumar Shaw and Kumar Pal [19] to report inter-domain distances in different pH-induced conformers of HSA. Also, the Trp fluorescence of TF overlap with the absorption spectrum of HSA–PPIX, and the absorption spectrum of HSA–PPIX overlaps with the fluorescence emission spectrum of HSA–PPIX. Hence, when excited at 297 nm, the fluorescence of PPIX-labeled HSA (HSA–PPIX) is negligible, whereas the fluorescence of TF is significant, making them a useful donor–acceptor pair to study their interactions. As illustrated in Fig. 4, when TF was added to the PPIX-labeled HSA solution, energy transfer was observed at 640 nm, which suggests that two proteins came in close contact and could interact with each other. Using other techniques, we further investigated this interaction and the role of LMF in this interaction.

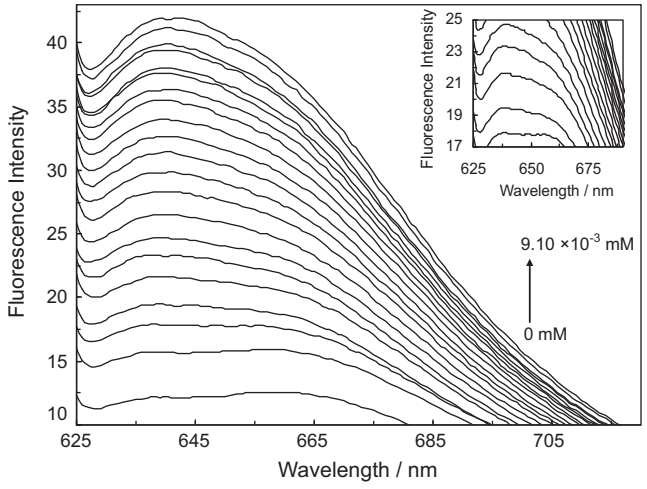


**Fig. 4.** Effect of TF on fluorescence spectra of PPIX-labeled HSA at 640 nm. Phosphate buffer; $T$ = 298 K; pH 7.4.

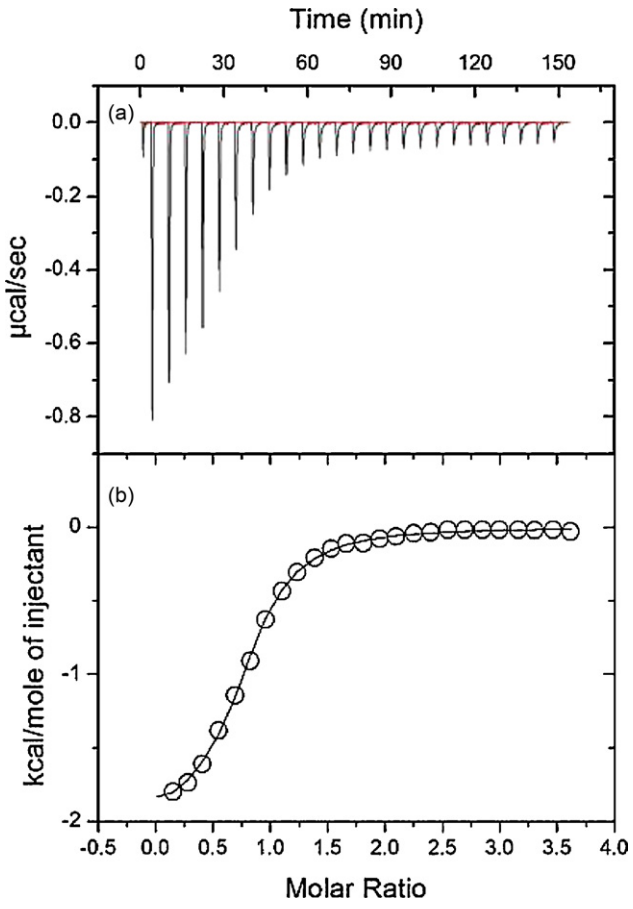


**Fig. 5.** ITC measurements of the binding of TF to HSA at 25 °C. (a) Heat of injection of ($3.7 \times 10^{-3}$ mM) TF into a cell containing ($4 \times 10^{-3}$ mM) HSA. (b) Integrated heat evolved per mole of TF added corrected for the heat of dilution against the molar ratio of TF to HAS. Data (○) were fitted to a single-site binding model and the solid line represents the best fit.

### 3.5. ITC

ITC was used to directly evaluate the effect of the drug on the thermodynamics of the interaction of TF with HSA. Fig. 5a shows the ITC curve of the interaction of TF with HSA (corrected by subtraction of the heat of dilution) in the absence of drug at 25 °C. All peaks were downward, indicating that the reactions were mainly exothermic. The respective binding isotherm is shown in Fig. 5b. Similar graphs were obtained for different concentrations of drug at 25 °C. The calorimetric data were fitted to single-site binding equations (Table 1). From Table 1 it can be deduced that, in the absence of LMF, the reaction was mainly entropy-driven even though enthalpy and entropy were favorable and electrostatic interactions were dominant. However, by enhancement of LMF concentrations, binding was becoming more enthalpy-driven with favorable enthalpy and unfavorable entropy in such a way that van der Waals forces and hydrogen bonding became dominant [26]. Interestingly, in the presence of drug, entropy was decreased. A plausible explanation could be that, upon drug association, protein molecules undergo conformational changes in such a way that their flexibility is increased. That is, proteins are more flexible with more

**Table 1**
Thermodynamic parameters of the interaction between TF and HSA in the presence and absence of LMF at 298 K, pH 7.4.

| LMF (mM) | $K \times 10^{-6}$ (L mol$^{-1}$) | $n$ | $\Delta H^0$ (kcal mol$^{-1}$) | $\Delta S^0$ (cal mol$^{-1}$ K$^{-1}$) | $T\Delta S^0$ (kcal mol$^{-1}$) | $\Delta G^0$ (kcal mol$^{-1}$) |
|---|---|---|---|---|---|---|
| 0 | 0.68 ± 0.01 | 0.88 | −0.64 ± 0.01 | 24.59 ± 0.01 | 7.57 ± 0.01 | −8.21 ± 0.01 |
| 0.001 | 1.06 ± 0.01 | 0.76 | −1.77 ± 0.01 | 21.83 ± 0.01 | 6.72 ± 0.01 | −8.49 ± 0.01 |
| 0.002 | 4.49 ± 0.02 | 2.18 | −13.86 ± 0.02 | −14.54 ± 0.02 | −4.48 ± 0.02 | −9.38 ± 0.02 |

conformations before association and are forced to assume a single conformation after formation of protein–protein complexes. This will result in an unfavorable decrease in entropy [21]. Table 1 also shows that the $\Delta G^0$ value become more negative in the presence of drug which suggests the interaction was become more spontaneous and that the binding constant at TF binding to HSA becomes stronger in the presence of LMF. Table 1 shows that the value of $n$ was increased in the presence of drug from ~1 to 2, suggesting a stoichiometry of 1:1 to 1:2 in the absence and presence of drug, respectively.

### 3.6. ANS fluorescence

ANS is barely fluorescent in aqueous solutions but, if bound to the hydrophobic portions of proteins, its fluorescence increases significantly, which makes it a useful hydrophobic probe [27]. Hydrophobic interaction plays a major part in PPI, so investigating the effect of LMF on the hydrophobicity of each protein is important. In this regard, LMF was added to the mixture of HSA–ANS and TF–ANS and ANS fluorescence recorded. The enhancement in ANS fluorescence for both proteins was small. However, for TF this was more significant, suggesting that the drug molecules could interact with both proteins and increase the exposure of hydrophobic pockets. Also, the fluorescence enhancement was measured for the mixture of HSA–TF and was shown to overlap with that of their algebraic average (Fig. 6). This indicates that hydrophobic interactions probably play a minor part in PPI, which further confirms the results obtained from ITC.

### 3.7. RLS

The RLS spectra of HSA upon titration by TF, in the presence and absence of LMF, were recorded by synchronous scanning from 220 nm to 700 nm with $\Delta\lambda = 0$ nm. Fig. 7a shows the spectra in the absence of LMF whereas Fig. 7b compares the results as a function of LMF concentration. Upon addition of TF to HSA, a remarkable increase in RLS was observed and LMF could further enhance the observed effect. It is known that RLS enhancement could be the result of enlargement of the molecular volume of the complexes, as can be inferred from the RLS formula of [28]:

$$I = \frac{32\pi^3 V^2 n^2 N}{3\lambda_0^4}[(\delta_n)^2 + (\delta_k)^2] \quad (3)$$

where $n$ is the refractive index of the medium, $N$ is the molarity of the solution, $\lambda_0$ is the wavelength of incident and scattered, $\delta_n$ and $\delta_k$ are the fluctuations in the real and imaginary components of the refractive index of the particles, respectively, and $V$ is molecular volume. When other factors are fixed, the RLS enhancement is directly proportional to the square of the molecular volume. Bear-

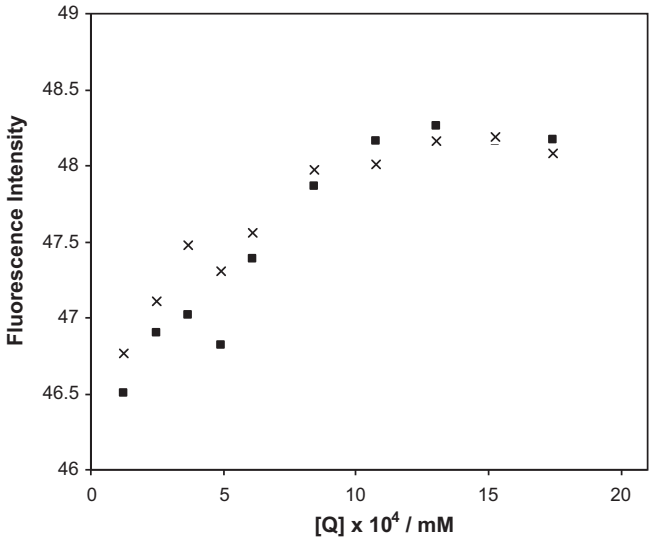


**Fig. 6.** ANS fluorescence enhancement as a function of LMF concentration for HSA–TF (rectangles) and algebraic average of HSA–TF (cross). LMF concentration was varied from 0 mM to 0.002 mM, with an ANS concentration constant of 0.005 M. Concentrations of HSA, TF and HSA–TF were $4.5 \times 10^{-3}$ Mm, $3.7 \times 10^{-3}$ mM and $4.5 \times 10^{-3}$ mM, respectively.

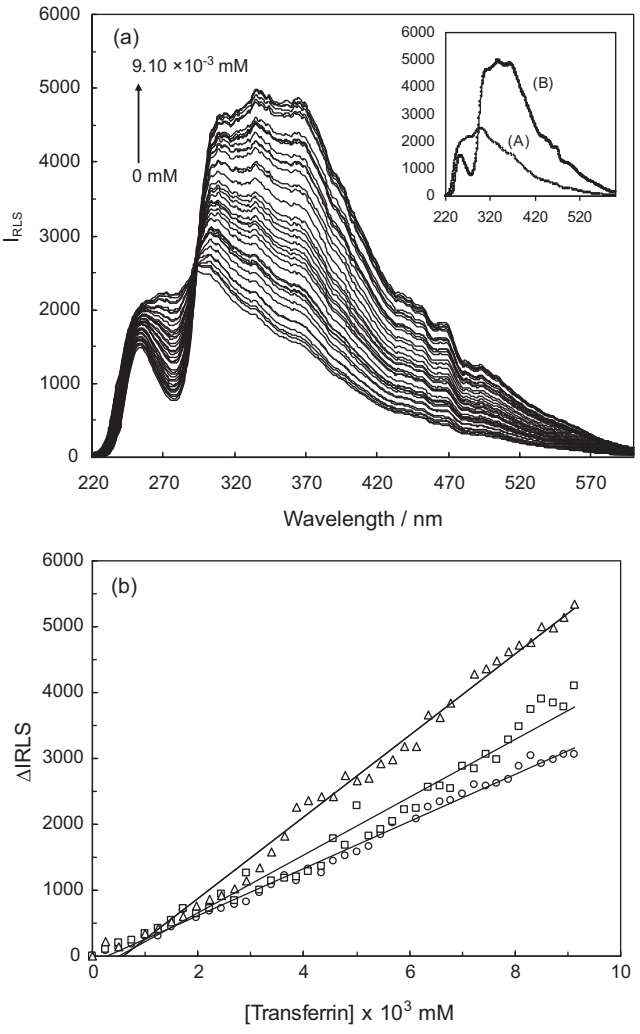


**Fig. 7.** (a) RLS spectra of the HSA–TF system. Inset shows the HSA (A) and HSA–TF complex (B). (b) RLS enhancement as a function of TF concentration in the absence (open circles), and presence of 0.001 mM (squares), 0.002 mM (triangles) LMF. TF concentration varied from 0.25 μM to 9.10 μM [HSA] = 4 μM.

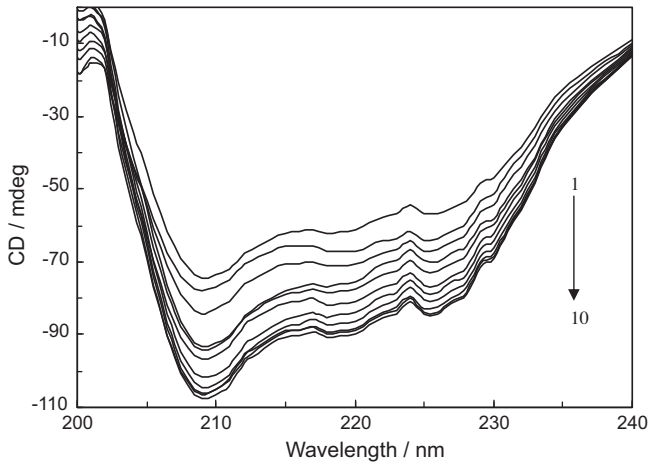


**Fig. 8.** Far-UV CD spectra of HSA upon binding to TF. TF/HSA molar ratios of 0–2.28.

ing these points in mind, it is deciphered from the results that the added TF may interact with HSA, forming a new HSA–TF species with a larger size than that of HSA and TF, separately. Also, LMF could enhance these complex formations. Thus, the more increased RLS signal observed under the given conditions.

### 3.8. CD spectroscopy

CD spectroscopy in far-UV regions allows an effective analysis of changes in the secondary structure of proteins upon interaction with ligands or other proteins in solution [29]. Changes in the secondary structural contents of HSA and TF upon interaction with different concentrations of LMF were calculated. The α-helical content decreased in the order 5.66 ± 0.03% and 4.92 ± 0.03%, the β-sheet content increased in the order 1.75 ± 0.02% and 2.2 ± 0.01%, the turns were 1.99 ± 0.01% and 1.19 ± 0.02%, and the unordered coils were 1.92 ± 0.01% and 1.53 ± 0.01% for HSA and TF, respectively.

Fig. 8 shows the CD spectra of HSA titrated by TF. They exhibit double minima at 208 and 222 nm, respectively, which is characteristic of high α-helical content. Moreover, the values of these negatives bands at 208 nm and 222 nm increased regularly, which suggested the gain of α-helical content in both proteins after complex formation [29]. Similar graphs were obtained in the presence of 0.001, 0.0015, and 0.002 mM LMF (data not shown) and secondary structural changes measured. Change in secondary structure upon titration of TF to HSA, was estimated where the α-helix content and unordered coil (except for the absence of LMF) tended to increase, and β-sheet and turn content tended to decrease. To illustrate the effect of LMF on structural changes in proteins upon PPI, the slopes of previous curves were plotted as a function of LMF concentration (data not shown). It was found that LMF weakened and strengthened the formation of the α-helix and unordered coiled formation, respectively, upon PPI. Also, it weakened and strengthened the turns and β-sheet destructions, respectively.

### 3.9. Protein homology modeling

To gain insight into the mode of interaction of TF with HSA, a homology-based model of human holo-TF was constructed (as explained in Section 2). The final refined conformer of human holo-TF had an ERRAT score of 87.275. It was also validated by the Ramachandran plot, which showed 539 residues (90.7%) in the most favored region with 4 (0.7%) residues in additional allowed regions. The Ramachandran plot is constructed for models based on an analysis of 118 structures of resolution of ≥2.0 Å and *R*-factor ≤20%. A good-quality model would be expected to have >90% in the most-favored regions. Therefore, the results were all in the acceptable range.

### 3.10. Molecular modeling

To acquire more information about the interaction of TF with HSA, interaction models were generated using molecular modeling. Having determined the most plausible binding sites of LMF on each protein separately, followed by energy-minimization steps, protein–protein docking was initiated. Identical procedures were carried out on LMF-free proteins. The best docking result of interaction between TF and HSA in the absence and presence of LMF is shown in Fig. 9a and b: the binding sites of drugs were not located within the interface of the protein–protein complex. A plausible reason for the observation that the "*n*" value for mixtures of HSA and TF is lower than that in their algebraic average (see Section 3.1) could be caused by the induced structural transition in the drug binding sites upon PPI, and may not be generated by positioning of the binding sites in the interface. Moreover, it can be deciphered that HSA and TF have different modes of interaction in

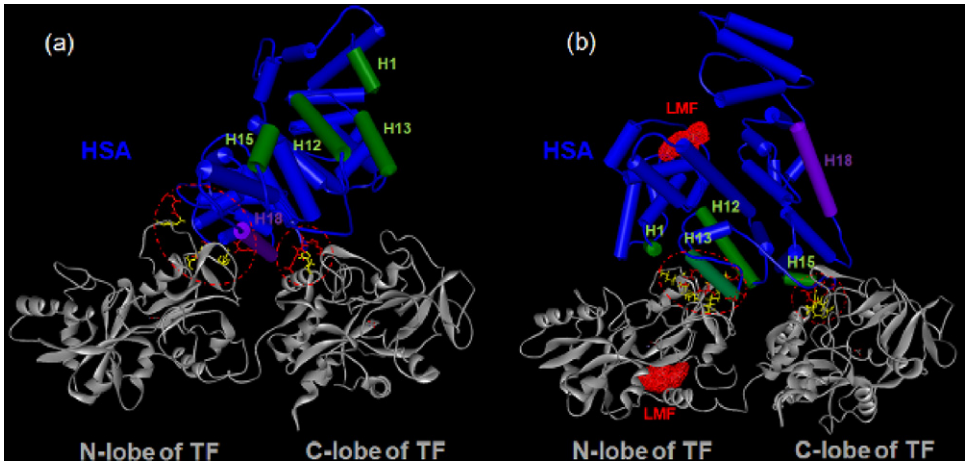


**Fig. 9.** Model of HSA–TF interaction in the absence (a) and presence (b) of LMF. HSA is represented by a schematic view, colored in blue. The helices which contribute the most in the interaction with TF in the absence and presence of LMF are colored violet and green, respectively. TF structure (obtained by homology modeling) is represented by a ribbon, colored in gray. The position of docked LMF to each protein is highlighted by surface representation of LMF, colored in red. The red rings show the area of hydrogen bonding at the interface which stabilizes the HSA–TF interaction. The amino acids of HSA and TF involved in hydrogen bonding are colored in red and yellow, respectively. (For interpretation of the references to color in this figure legend, the reader is referred to the web version of the article.)

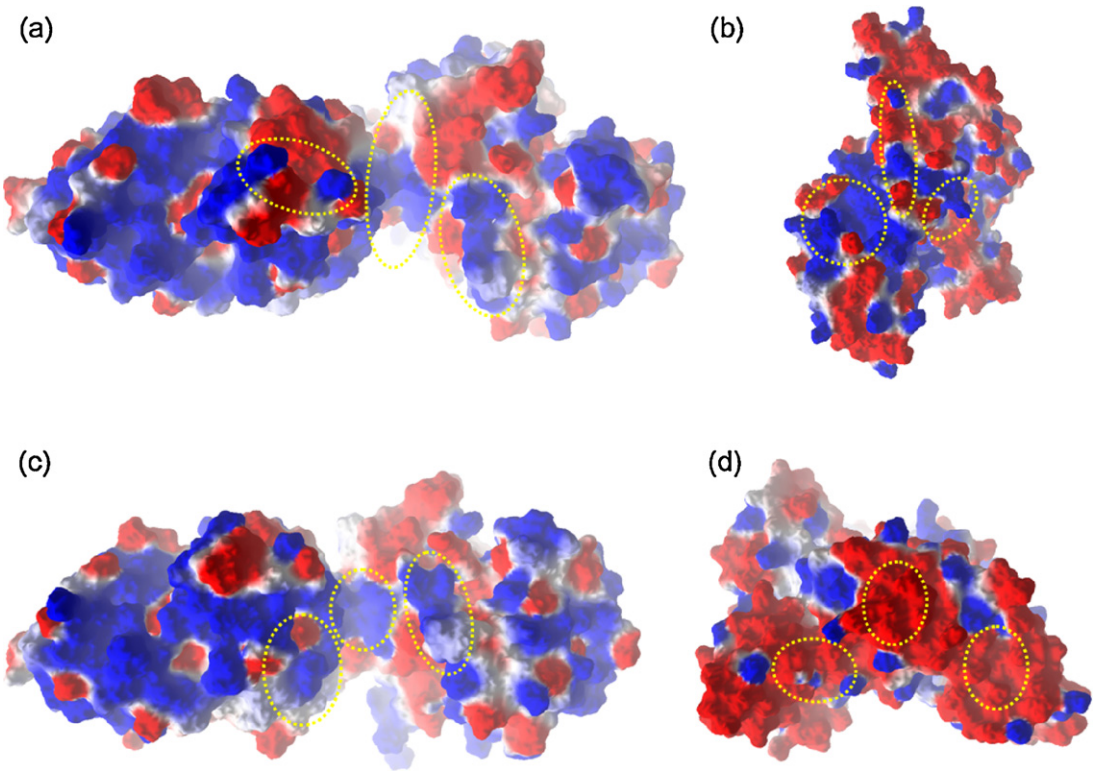


**Fig. 10.** Representations of electrostatic potential on the molecular surface of TF (a) and of HSA (b) in the absence of LMF; and of TF (c) and HSA (d) in the presence of LMF. Blue and red colors represent the positive and negative potentials calculated using the Molegro Molecular Viewer program, respectively. The circle shows the surface area involved in the interaction.

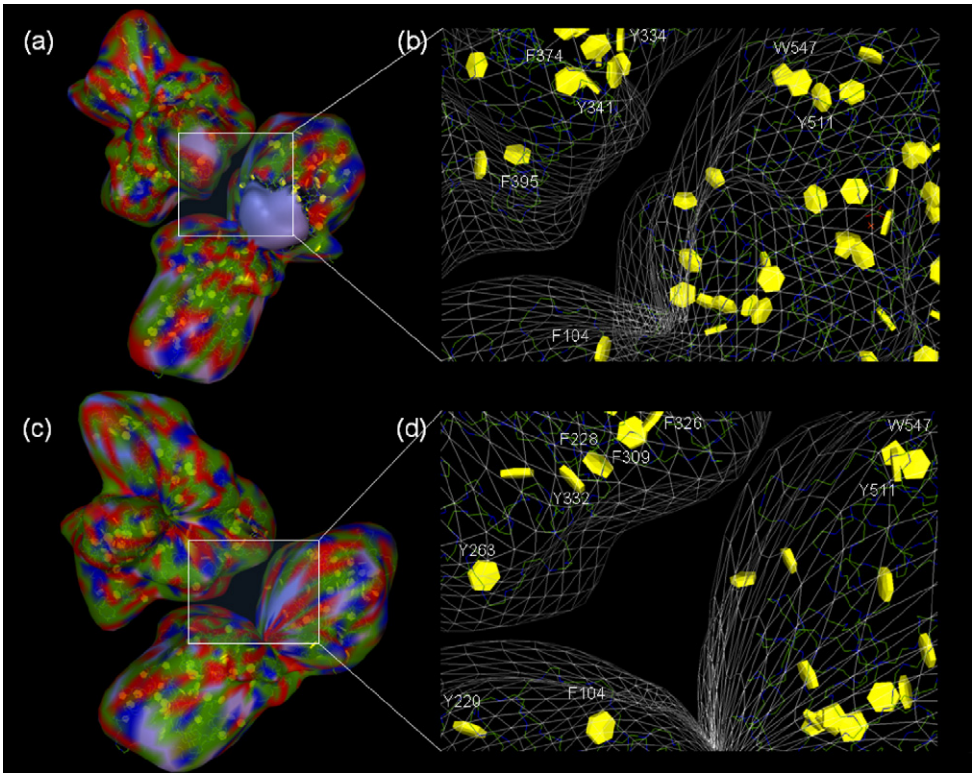


**Fig. 11.** Spatial distribution of aromatic amino acids represented by a polygon, colored in red, in the HSA–TF complex model. Panel (a) shows the transparent spherical harmonic surfaces to order $L = 12$ colored by atoms for the HSA–TF model in the absence of LMF and panel (c) in the presence of LMF. The most important intrinsic fluorophore residues [Trp (W), Tyr (Y) and Phe (F)] involved at the interface of the complex in the absence and presence of LMF are shown in panels (c) and (d), respectively. In each panel, the left molecule is HSA and the right molecule is TF (the N-lobe is downward whereas the C-lobe is upward).

**Table 2**
Hydrogen bonding at the interface of the TF–HSA model in the presence of LMF.

| HSA | TF | |
|---|---|---|
| Asp 269 | N-lobe | Lys 113 |
| Glu 266 | | Gly 197 (1.23 Å) |
| Lys 262 | | Leu 192 (2.35 Å and 2.35 Å), Lys 193 (1.03 Å, 0.83 Å, 1.46 Å) |
| Lys 233 | | Lys 100 (1.87 Å, 2.13 Å), Asp 101 (2.54 Å, 1.81 Å), Ser 102 (2.13 Å) |
| Asp 308 | C-lobe | His 347 (1.57 Å) |
| Asp 301 | | Glu 504 (214 Å), Asn 506 (1.92 Å) |
| Ser 312 | | Glu 622 (1.61 Å) |

**Table 3**
Hydrogen bonding at the interface of the TF–HSA model in the absence of LMF.

| HSA | TF | |
|---|---|---|
| Glu 495 | N-lobe | Lys 214 (1.93 Å, 2.15 Å) |
| Lys 541 | | Glu 234 (1.73 Å, 2.27 Å, 2.12 Å, 2.23 Å) |
| Gln 390 | | Arg 229 (2.28 Å and 1.46 Å) |
| Lys 439 | C-lobe | Glu 354 (2.28 Å) |
| Glu 442 | | His 346 (2.32 Å, 2.02 Å, 1.02 Å) |
| Ala 443 | | His 346 (2.33 Å, 2.17 Å, 1.57 Å) |

the absence and presence of LMF. In the absence of LMF, helix 18 (H18) of HSA contributes the most in the HSA–TF interaction. However, in the presence of LMF, four helices (H1, H12, H13 and H15) of HSA are more involved in this interaction. Another difference which can be observed in Fig. 9a and b is in the number and type of amino acids involved in the hydrogen bonding between HSA and TF (Tables 2 and 3). The number of hydrogen bonds is higher in the presence of LMF.

The electrostatic surface potential of the two proteins in the presence and absence of LMF calculated by Molegro Molecular Viewer® (http://www.molegro.com/mmv-product.php) is shown in Fig. 10. From an electrostatic viewpoint, the interaction surfaces of HSA and TF are complementary. This, and the prediction that the HSA–TF complex is stabilized by hydrogen bonding, is in agreement with the results obtained from ITC experiments.

The spatial distribution of intrinsic fluorophore residues of proteins in the absence and presence of LMF was inspected using "aromatic ring polygons" representations under "solid models control panel" of HEX 5.1® (Fig. 11a–d). In the absence of LMF (Fig. 11a and b) Trp 547, Tyr 511, and Phe 104 of TF; and Tyr 341, Tyr 344, Phe 374, and Phe 395 of HSA were located in the interface. However, in the presence of LMF (Fig. 11c and d), the Trp 547, Tyr 511, Tyr 220 and Phe 104 of TF; and Tyr 332, Tyr 263, Phe 228, Phe 309 and Phe 326 of HSA were located in the interface. This suggests that the reason for the observed higher blue-shifted $\lambda_{em,max}$ (Fig. 2a) and value of $H$ (Fig. 3c) for the mixture of HSA and TF compared with their algebraic average is because of sequestration of these residues from the solvent and their positioning in the interface.

## 4. Conclusion

Combining the results obtained with intrinsic fluorescence, second-derivative fluorescence, synchronous fluorescence spectroscopy, FRET, ITC, ANS fluorescence, RLS, CD as well as molecular modeling, it has been shown that LMF-induced conformational changes could promote the interaction between HSA and TF.

In the absence of LMF, HSA could interact with TF to form a new species with a larger size than each protein partner. The nature of this interaction was mostly electrostatic, but other interactions such as hydrogen bonding could not be neglected. This interaction was accompanied by structural changes in proteins as evidenced by CD, which can modify the binding interaction of LMF to them.

The presence of LMF could induce conformational transitions in both proteins in such a way that the nature of HSA–TF interactions became mainly based on hydrogen bonding and van der Waals forces. LMF could also strengthen the HSA–TF interaction. These data provide better understanding of the mechanism underlying the emergence of the side effects of antibiotics. That is, these phenomena could cause interference with the natural function of both proteins. For example, a probable reason for edema observed as a side effect of LMF could be due to the strengthening effect of LMF on HSA–TF or the interaction of HSA with other plasma proteins in such a way that they form aggregates and their subsequent elimination could reduce the HSA concentration. This could result in reduction of the colloidal osmotic pressure in plasma and eventually to edema. However, clinical investigations are required to prove this hypothesis. Also our results have important roles in diagnostic tests in which serum proteins are used as biomarkers, because drug intake may modify PPI in serum and this may lead to false-negative and false-positive results. Moreover, this investigation highlights the effect of other serum proteins on evaluation of the binding parameters of different ligands to other proteins in serum. This is due to the observation that the number of binding sites is lower for a mixture of proteins compared with their algebraic average. Taken together, the present study revealed the effect of antibiotics such as LMF in modification of serum PPI using HSA–TF as a model system.

## Acknowledgments

The financial support of the Research Council of the Islamic Azad University-Mashhad Branch is gratefully acknowledged. We also thank the Bioinformatics Laboratory of the Mashhad School of Pharmacy for their warm and helpful cooperation. The authors appreciate to Springer English editing service for the native English editing.

## References

[1] G. Schreiber, Kinetic studies of protein–protein interactions, Curr. Opin. Struct. Biol. 12 (2002) 41–47.
[2] H. Ruffner, A. Bauer, T. Bouwmeester, Human protein–protein interaction networks and the value for drug discovery, Drug Discov. Today 12 (2007) 709–716.
[3] K. Blennow, M.J. de Leon, H. Zetterberg, Alzheimer's disease, Lancet 368 (2006) 387–403.
[4] M. Bucciantini, E. Giannoni, F. Chiti, F. Baroni, L. Formigli, J. Zurdo, N. Taddei, G. Ramponi, C.M. Dobson, M. Stefani, Inherent toxicity of aggregates implies a common mechanism for protein misfolding diseases, Nature 416 (2002) 507–511.
[5] A.S. Rosenberg, Effects of protein aggregates: an immunologic perspective, AAPS J. 8 (2006) E501–E507.
[6] S. Ventura, Sequence determinants of protein aggregation: tools to increase protein solubility, Microb. Cell Factories 4 (2005) 1–8.
[7] C.O. Anderson, J.F.M. Niesen, H.W. Blanch, J.M. Prausnitz, Interactions of proteins in aqueous electrolyte solutions from fluorescence anisotropy and circular-dichroism measurements, Biophys. Chem. 84 (2000) 177–188.
[8] M. Nigen, V.L. Tilly, T. Croguennec, D. Drouin-Kucma, S. Bouhallab, Molecular interaction between apo or holo α-lactalbumin and lysosyme: formation of heterodimers as assessed by fluorescence measurements, Biochim. Biophys. Acta 1794 (2009) 709–715.
[9] M. Zhou, D.A. Lucas, K.C. Chan, H.J. Issaq, E.F. Petricoin III, L.A. Liotta, T.D. Veenstra, T.P. Conrads, An investigation into the human serum interactome, Electrophoresis 25 (2004) 1289–1298.
[10] S.H.C. Ip, G. Ackers, Thermodynamic studies on subunit assembly in human hemoglobin. Temperature dependence of the dimer–tetramer association constants for oxygenated and unliganded hemoglobins, J. Biol. Chem. 252 (1977) 82–87.
[11] L. Soltes, M. Mach, Estimation of drug–protein binding parameters on assuming the validity of thermodynamic equilibrium, J. Chromatogr. B: Anal. Technol. Biomed. Life Sci. 768 (2002) 113–119.
[12] D.C. Hooper, J.S. Wolfson, Quinolone Antimicrobial Agent, 2nd ed., American Society of Microbiology, Washington, DC, USA, 1993.
[13] H. Vahedian-Movahed, M.R. Saberi, J. Chamani, Comparison of binding interaction of lomefloxacin to serum albumin and serum transferrin by resonance Rayleigh scattering and fluorescence quenching methods, J. Biomol. Struct. Dyn. 28 (2011) 483–502.
[14] T.J. Peters, All About Albumin. Biochem, Genetics and Medical Application, Academic Press, San Diego, CA, 1996.

[15] P.T. Gomme, K.B. McCann, Transferrin: structure, function and potential therapeutic actions, Drug Discov. Today 10 (2005) 267–273.
[16] S.M. Shapiro, Bilirubin toxicity in developing nervous system, Pediatr. Neurol. 29 (2003) 410–421.
[17] A.C. Guyton, J.E. Hall, Textbook of Medical Physiology, 11th ed., Elsevier Health Sciences, 2006.
[18] J.R. Lakowicz, Principle of Fluorescence Spectroscopy, Springer Science+Business Media, New York, 2006, pp. 52, 277 and 530.
[19] A. Kumar Shaw, S. Kumar Pal, Resonance energy transfer and ligand binding studies on pH-induced folded states of human serum albumin, J. Photochem. Photobiol. B 90 (2008) 187–197.
[20] D.W. Ritchie, G.J.L. Kemp, protein docking using spherical polar Fourier correlations, Proteins 39 (2000) 178–194.
[21] M.B. Jackson, Molecular and Cellular Biophysics, Cambridge University Press, 2006.
[22] A. Mazo-Villarias, Second derivative fluorescence spectroscopy of tryptophan in proteins, J. Biochem. Biophys. Methods 50 (2002) 163–178.
[23] V. Kumar, V.K. Sharma, D.S. Kalonia, Second derivative tryptophan fluorescence spectroscopy as a tool to characterize partially unfolded intermediate of proteins, Int. J. Pharm. 294 (2005) 193–199.
[24] J.B.F. Lloyd, synchronized excitation of fluorescence emission spectra, Nature 231 (1971) 64–65.
[25] L. Stryer, Fluorescence energy transfer as a spectroscopic ruler, Annu. Rev. Biochem. 47 (1978) 819–846.
[26] P.D. Ross, S. Subramanian, Thermodynamics of protein association reactions: forces contributing to stability, Biochemistry 20 (1981) 3096–3102.
[27] L. Stryer, The interaction of a naphthalene dye with apomyoglobin and apohemoglobin: a fluorescent probe of non-polar binding sites, J. Mol. Biol. 13 (1965) 482–495.
[28] J. Anglister, I.Z. Steinberg, Depolarized Rayleigh light scattering in absorption bands measured in lycopene solution, Chem. Phys. Lett. 65 (1979) 50–54.
[29] H. Fu, Protein–protein interactions: methods and applications, in: Circular Dichroism Analysis for Protein–Protein Interactions, Springer, 2004 (Chapter 3).
[30] Y.L. Zhuo, J.M. Liao, F. Du, Y. Liang, Thermodynamics of the interaction of xanthine oxidase with superoxide dismutase studied by isothermal titration calorimetry and fluorescence spectroscopy, Thermochim. Acta 426 (2005) 173–178.